Romanian
NEUROSURGERY

rCBV and ADC based grading of gliomas with glimpse into radiogenomics

Seema Rohilla,
Ambresh R. Deodurg,
Pritviraj S. Kanakavvanavar,
Ishwar Singh,
Veena Gupta,
Dhara B. Dhaulakhandi

rCBV and ADC based grading of gliomas with glimpse into radiogenomics

Seema Rohilla[1], Ambresh R. Deodurg[1], Pritviraj S. Kanakavvanavar[1], Ishwar Singh[2], Veena Gupta[3], Dhara B. Dhaulakhandi[4]

[1] Department of Radiodiagnosis & Imaging. Post Graduate Institute of Medical Sciences, Pt. B.D. Sharma University of Health Sciences, Rohtak, INDIA

[2] Department of Neurosurgery. Post Graduate Institute of Medical Sciences, Pt. B.D. Sharma University of Health Sciences, Rohtak, INDIA

[3] Department of Pathology. Post Graduate Institute of Medical Sciences, Pt. B.D. Sharma University of Health Sciences, Rohtak, INDIA

[4] Department of Biotechnology & Molecular Medicine. Regional Cancer Centre. Post Graduate Institute of Medical Sciences, Pt. B.D. Sharma University of Health Sciences, Rohtak, INDIA

✉

Corresponding author:
Seema Rohilla

Post Graduate Institute of Medical Sciences, Sharma University of Health Sciences, Rohtak, India

seemarohilla@yahoo.co.in

ABSTRACT

Purpose. The present study was carried out to study the role of relative cerebral blood volume (rCBV), apparent diffusion coefficient (ADC) and MR spectroscopy in grading gliomas to help the surgeon plan the approach and extent of surgery as well as judge the need for any adjuvant radio/chemotherapy.

Methods. 65 patients with glioma were prospectively studied with MRI. Basic MR sequences (T1W, T2W, T2W/FLAIR) were followed by diffusion-weighted (DW) imaging with b value of 1000 (minimum ADC values used for analysis). Then the patients were administered Gadobenate Dimeglumine/ Meglumine Gadoterate in a dose of 0.1mmol/kg at a rate of 4ml/sec after which 20ml of saline was flushed at a rate of 4ml/sec and T2*W/FFE dynamic images were acquired; dynamics showing maximum fall in the intensity were used for creating rCBV and rCBF maps and calculating rCBV. Single voxel spectroscopy (SVC) was done using the PRESS sequence with intermediate TE of 144ms. NAA/Cr, Cho/Cr, Cho/NAA, Cho+Cr/NAA and NAA/Crn ratios (NAA from the tumour, Crn from the normal side) were calculated.

Results. Grade I gliomas showed minimum ADC>0.84×10^{-3}mm^2/s and maximum rCBV<1.9ml/100gm, grade II gliomas showed min ADC 0.75-0.84×10^{-3}mm^2/s and max rCBV of 1.9-2.6ml/100gm, grade III had min ADC of 0.70-0.75×10^{-3}mm^2/s and max rCBV of 2.7-3.0ml/100gm, while grade IV tumours showed min ADC<0.70×10^{-3}mm^2/s and max rCBV>3.0ml/100gm. rCBV values were better than ADC values in differentiating grade I from II and grade II from III. The ADC values were better than rCBV values in differentiating grade III from grade IV.

Conclusions. Both minimum ADC and maximum rCBV within the tumour were significant but these parameters within peritumoural oedema were not significant in grading gliomas. Though lipid and lactate (especially lipid) peaks were found more frequently in higher-grade tumours, various spectroscopy parameters were not significant in grading gliomas. Preoperative grading of gliomas with the help of

advanced MR parameters like ADC and rCBV can help the surgeon plan the approach and extent of surgery as well as judge the need for any adjuvant radio/chemotherapy. Advancing radio-genomic and radiomic technologies can supplement the current radiologic methods of diagnosis and prognosis.

INTRODUCTION

The majority of primary brain tumours are gliomas which may be low (grade I and II) or high (grade III and IV) grade [1]. The inherent heterogeneity of gliomas makes it difficult to grade them with conventional MRI. However, advanced MRI techniques such as perfusion, diffusion, spectroscopy and largely experimental molecular imaging can aid in such grading.

Dynamic susceptibility contrast magnetic resonance (DSC-MR) imaging helps in assessing tumour vascularity and angiogenesis non-invasively by way of decrease in signal intensity with time during the first pass of a bolus of paramagnetic contrast agent. The maximum tumour rCBV tends to increase as the grade of astrocytoma increases. Increased cell density reduces Brownian motion leading to restricted diffusion and reduced ADC. Thus, higher the tumour grade, lower the ADC. In a tumour, the increase in cell turnover leads to an increase in choline concentration, along with a depression of the NAA peak due to loss of healthy glioneural structures. Lactate peak suggests hypoxia while lipid peak is suggestive of necrosis, an indicator of malignancy.

Preoperative grading of gliomas with the help of advanced MR parameters like ADC and rCBV (specially in hospital settings which lack stereotactic biopsy facility) can help surgeon plan the approach and extent of surgery as well as judge the need of any adjuvant radio/chemo therapy. Relationship between imaging features and genetic/molecular features of tumours can be addressed using radio-genomic methods. Continuously evolving "omics" procedures and modalities coupled with advances in basic tumour biology, histopathology, computational and molecular tools can complement imaging as well as genetic analysis. Integration of imaging markers derived from clinical images and genomic markers such as EGFR, MGMT, IDH1, 1p/19q codeletion can be explored in a non-invasive manner [2]. For example, a direct association is found in EGFR amplification and contrast enhancement in GBM; ill-defined tumour margins and tumour heterogeneity can potentially be used as imaging biomarkers for 1p/19q codeletion in gliomas [3]. Application of radiogenomic markers is particularly useful when taking biopsy is not possible. To have a deeper insight into tumour makeup, a wide array of quantitative and qualitative imaging features may be utilized to record distinct imaging phenotypes and link them to genomic profiles. Whereas staging signifies the tumour spread, grading signifies the general tumour aggressiveness. Hybrid of imaging and genomic techniques have not only led to improved tumour grading assessment by capturing heterogeneity more precisely but have also added refinement to staging. Various radiological features like location, lateralization, enhancement characteristics, perfusion parameters, ADC, etc. can help assess genetic/molecular make-up to some extent which further help in predicting prognosis and effectiveness of therapy. Current and evolving radio-genomic, proteomic and spectroscopic technologies can supplement the current radiologic methods and procedures to help clinicians better equip for making accurate diagnosis and precisely grade gliomas.

MATERIAL AND METHODS

65 patients with glioma were evaluated. Basic MRI sequences i.e. T1W(TE-15 ms, TR-596 ms, field of view(FOV)-230 mm, matrix size-(186x256), flip angle-69o and NSA-1), T2W(TE-100 ms, TR-4431 ms, FOV-230 mm, matrix size-(236X512), flip angle-90o and NSA-2) and T2W/FLAIR(TE-120 ms, TR-6000 ms, FOV-230 mm, matrix size-(172x256), flip angle-100o TI(time to inversion)=2000 ms and NSA-1) were done in axial, sagittal and coronal plains as per requirement on Gyroscan Intera Nova gradient 1.5 Tesla Philips Imaging system, Best, Netherlands using a SENSE head coil (6 channel phased array coil). Informed consent was taken from the participants. Approval of the Dean, Faculty of Medicine and Allied Sciences was taken for the study which was conducted in accordance to provisions of Institutional Ethics Committee.

Diffusion weighted imaging (DWI) was carried out with a single shot echo planar imaging (EPI) sequence with a TE-89 ms, TR-2609 ms, FOV 230 mm, matrix size- 89x256, flip angle-90o and NSA-3, with a b value of 1000. ADC map was calculated by automated software on workstation (view forum version 5.1) and minimum ADC values used for analysis. The ADC

values were calculated in tumours in all 65 cases and in peritumoural edema 56 cases.

Perfusion weighted imaging (PWI). The patients were given gadobenate dimeglumine/ meglumine gadoterate in a dose of 0.1 mmol/kg at a rate of 4 ml/s followed by saline flush of 20 ml at a rate of 4 ml/s using pressure injector medrad spectrosolaris version 008.001-sa. T2*W/FFE dynamic sequence (TE-30 ms, TR-627 ms, FOV-230, matrix size-128x128, flip angle-40o and NSA -2) was acquired. rCBV and CBF maps were created on the dynamic showing maximum fall in signal intensity on first pass of contrast bolus. Maximum rCBV was calculated with the help of automated software on View Forum 5.1. The values were calculated in tumour in all 65 cases and in perirumoral edema in 35 cases.

Spectroscopy. Single voxel spectroscopy (SVC) was performed using PRESS sequence with intermediate TE of 144 ms. The voxel was placed at most dark area in ADC map/maximum enhancing area on contrast MRI (scalp and skull bones were excluded from the voxel). Two spectroscopy data sets were obtained - one from the most malignant appearing area of tumour and another from the corresponding normal white matter. NAA/Cr, Cho/Cr, Cho/NAA, Cho+Cr/NAA and NAA/Crn ratios- NAA from tumour, Crn from normal side were calculated.

Two sample Wilcoxon ranksum (Mann-whitney) test, Kruskal-Wallis equality-of-populations rank test and ROC analysis were the statistical tests applied with stata software version 11.2. Surgery/biopsy were used as gold standard for final diagnosis.

RESULTS

65 patients with glioma (4-76 years old with mean age of 41 year) with 49 males and 16 females were studied. Basic MR sequences showed tumour appearance on T1W, T2W, FLAIR, and contrast enhanced T1W images (Figures 1-3). Most of the tumours were hypointense on T1W and hyperintense on T2W images. High grade tumours were more heterogeneous and showed contrast enhancement. Haemorrhage and necrosis were more common in grade IV tumours. They were seen less frequently in grade II and grade III tumours, were almost equally frequent in grade II and grade III tumours and were not seen in grade I tumour. Mild

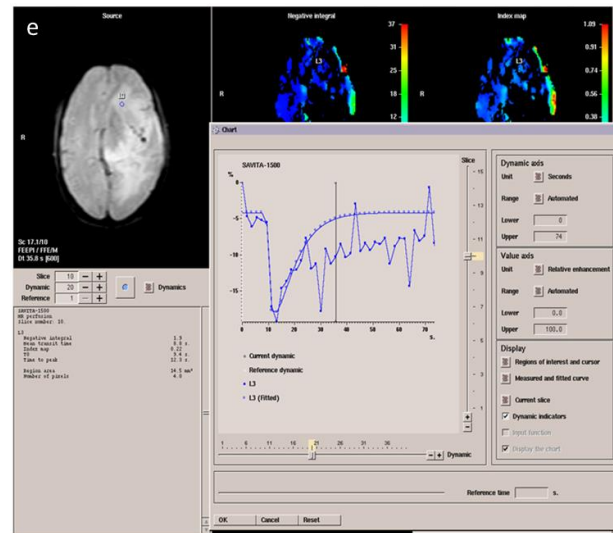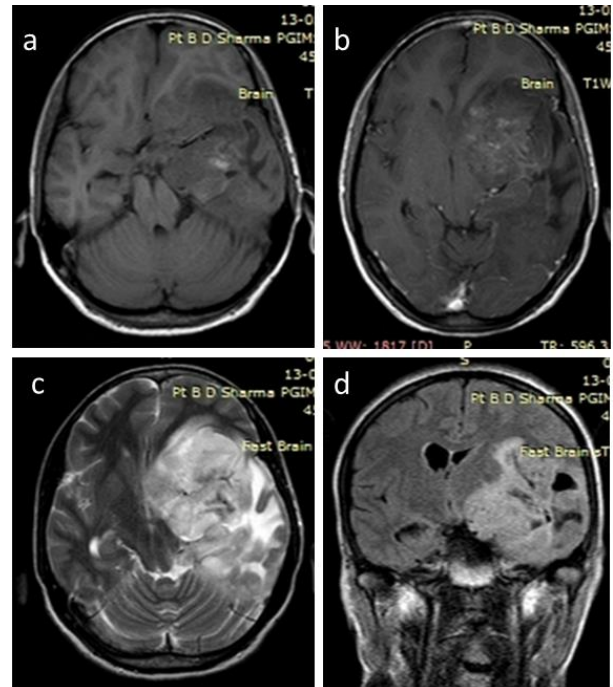enhancement could be seen in some low-grade gliomas also.

Figure 1. 40yr old female patient with oligodendroglioma in left frontotemporal region (Grade II):

(A) Axial T1W image showing illdefined hypointense lesion in left frontotemporal region showing area of hemorrhage as hyperintense signal and necrosis as hypointense signal.

(B) Axial T1W contrast image showing mild heterogenous contrast enhancement.

(C) Axial T2W image showing illdefined hyperintense lesion with minimal peitumoral edema.

(D) Coronal T2W/FLAIR image showing the lesion causing mass effect on surrounding parenchyma with midline shift towards right side.

(E) Axial T2*W first pass perfusion image showing color coded rCBV maps along with time-signal intensity curve and various parameters [rCBV (negative integral), rCBF (index map),MTT and TTP],rCBV being 1.9ml/100gm.

Even though the lesion appeared high grade on morphological features the parameters showed low grade and was proved to be grade II oligodendroglioma.
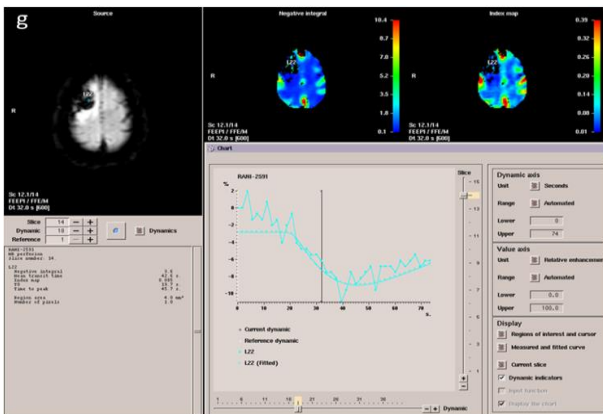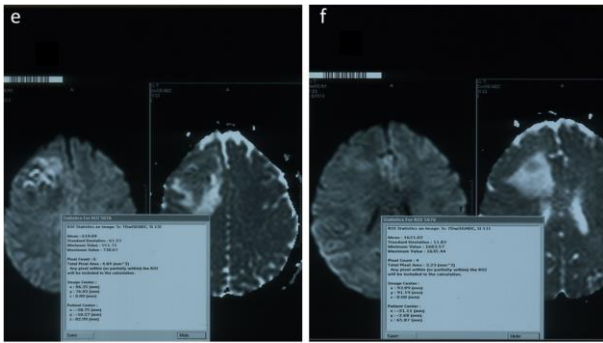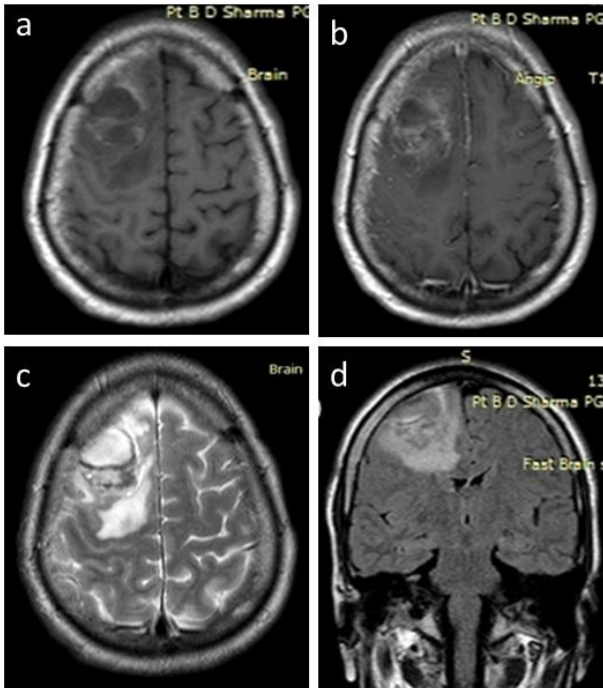

Figure 2. 52 yr old female patient with anaplastic astrocytoma in right frontal lobe (Grade III):

(A) Axial T1W image showingilldefinedhypointense lesion with hemorrhagic areas seen as hyperintense signal seen in right frontal lobe.

(B) Axial T1W contrast image showing mild heterogenous contrast enhancement.

(C) Axial T2W image showing the lesion as heterogeneously hyperintense and peritumoral edema as hyperintense signal.

(D) Coronal T2W/FLAIR image showing the hyperintense mass in right frontal lobe no significantmass effect noted.

(E) Axial diffusion weighted image showing patchy areas of diffusion restriction seen as hyperintense signal, corresponding area is seen as hypointense signal in ADC map. Minimum ADC value calculated was 0.614x10-3mm2/ sec.

(F) DWI and ADC maps showing minimum ADC value calculated from the peritumoraledema which was 1.621x10-3mm2/sec.

(G) Axial T2*W first pass perfusion Image showing color coded rCBV maps along with timesignal intensity curve and various parameters [rCBV (negative integral), rCBF (index map),MTT and TTP],rCBV being 3.6ml/100gm.
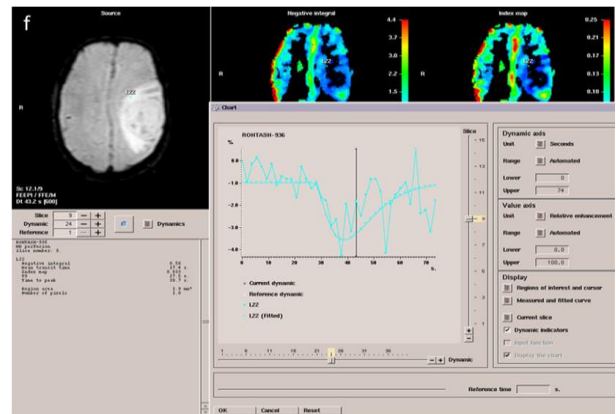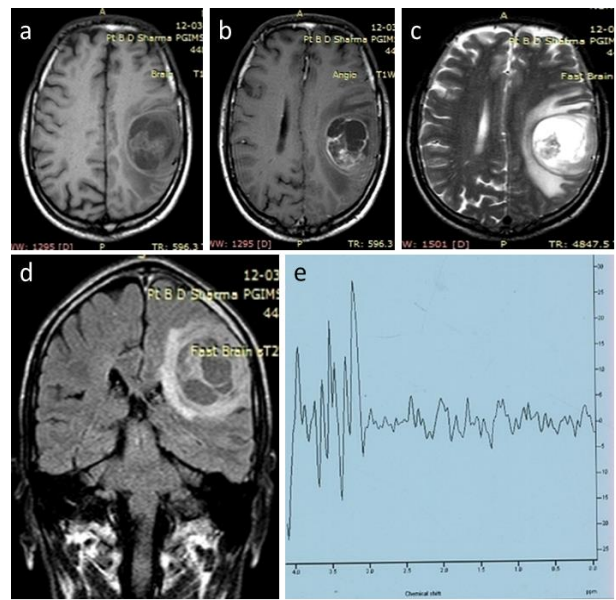
DWI

Tumour areas which showed diffusion restriction appeared hyperintense on DW images and hypointense on ADC maps. The ADC values obtained for different tumour grades were analysed.

DWI in tumour

Population rank test for ADC values in tumour according to different grades showed a probability of 0.0001(highly significant). Box plot showing distribution of ADC values with respect to grades is shown in Figure 4(A). ROC curve analysis is shown in Figure 4(B-D). The summary statistics [sensitivity, specificity, accuracy, area under the curve (AUC), standard error and 95% confidence interval for differentiating various grades based on different cut off values of ADC] are shown in Table 1. The range of ADC values for different tumour grades is as shown in Table 2.

DWI in peritumoural edema

Population rank test for ADC values in edema according to different tumour grades showed a p value of 0.4386. Since p value is more than 0.05 this parameter is not significant in assessing tumour grades.
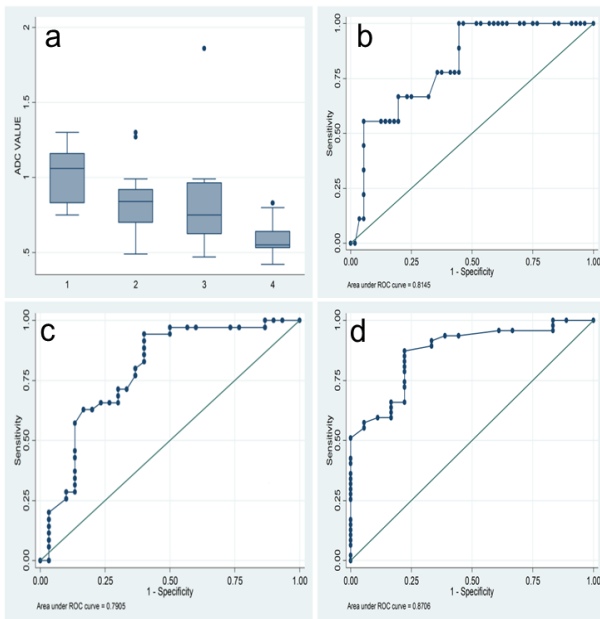

Figure 4.
a. Box plot showing distribution of ADC vaues;
b. ROC curves showing ADC values forgrade I v/s grade II;
c. ROC curves showing ADC values for grade II v/s grade III;
d. ROC curves showing ADC values for grade III v/s grade IV.

PWI

PWI in tumour

Population rank test for maximum rCBV values in tumour according to different grades showed a p value of 0.0002. Since p value is well below 0.05, the parameter was highly significant in grading tumours. Box plot showing distribution of maximum rCBV values in tumour with respect to various grades is shown in Figure 5(A). ROC curve analysis for this data is shown in Figure 5(B-D). The summary statistics [sensitivity, specificity, accuracy, AUC, standard error and 95% confidence interval for differentiating various grades based on different cut off values of rCBV] are shown in Table 1. The range of rCBV values in various grades is shown in Table 2.
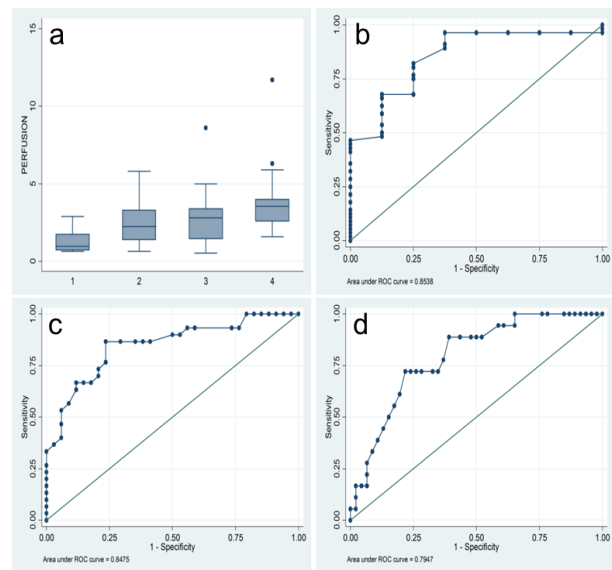
Figure 5.
a. Box plot showing distribution of rCBV values;
b. ROC curves showing rCBV values forgrade I v/s grade II;
c. ROC curves showing rCBV values forgrade for II v/s grade III;
d. ROC curve showing rCBV values for grade III v/s grade IV.

PWI in periumoural edema

Population rank test for maximum rCBV values in edema according to different grades showed a p value of 0.1362. Since the p value is well above 0.05, the parameter is not significant in grading tumours.

Percentage signal (%) drop in tumour

Another parameter obtained on perfusion studies is % drop in intensity. Kruskal-Wallis equality-of-populations rank test for %drop showed a p value of 0.0004. Since the p value is less than 0.05, %drop significantly co-related with tumour grade. Box plot

showing distribution of % drop values with respect to grades is shown in Figure 6(A). ROC curve analysis is shown in Figure 6(B-D). The summary statistics [sensitivity, specificity, accuracy, AUC, standard error and 95% confidence interval for differentiating various grades based on different cut off values of percentage drop] are shown in Table 1. The range of % drop values with respect to various grades is as shown in Table 2.

	Parameter	Cut Off Value	Sensitivity (%)	Specificity (%)	Accuracy (%)	Area Under the Curve	Standard Error	95% Confidence Interval
Grade I vs II	ADC Value	0.84×10^{-3} mm^2/s	66.67	67.86	67.69	0.8145	0.0684	0.68042-0.94855
	rCBV	1.9 ml/100 g	75	75	75	0.8538	0.0708	0.71500-0.99359
	Percentage Drop	9 %	88.24	100%	89.29	0.9255	0.0367	0.85354-0.99744
Grade II vs III	ADC Value	0.75×10^{-3} mm^2/s ($\times 10^{-3}$ mm^2/s	71.43	70	70.77	0.7905	0.0593	0.67434-0.90667
	rCBV	2.6 ml/100 g	76.67	76.47	76.56	0.8475	0.0493	0.75094-0.94415
	Percentage Drop	18 %	70.37	68.97	69.64	0.7618	0.0651	0.63425-0.88938
Grade III vs IV	ADC Value	0.70×10^{-3} mm^2/s	78.72	77.78	78.46	0.8706	0.0470	0.77853-0.96260
	rCBV	3 ml/100 g	72.22	71.74	71.87	0.7947	0.0584	0.68026-0.90911
	Percentage Drop	22 %	75	75	75	0.7937	0.0700	0.65665-0.93085

Table 1. Table showing summary statistics for different values of ADC, rCBV and percentage drop in relation to tumor grades.

Tumor Grade	ADC value ($\times 10^{-3}$ mm^2/s)	rCBV value (ml/100 g)	% Drop
Grade I	>0.84	<1.9	<9 %
Grade II	0.75-0.84	1.9-2.6	9-18 %
Grade III	0.70-0.75	2.7-3.0	19-22 %
Grade IV	<0.70	>3.0	>22 %

Table 2. Table showing range of ADC, rCBV and % drop values in various tumor grades
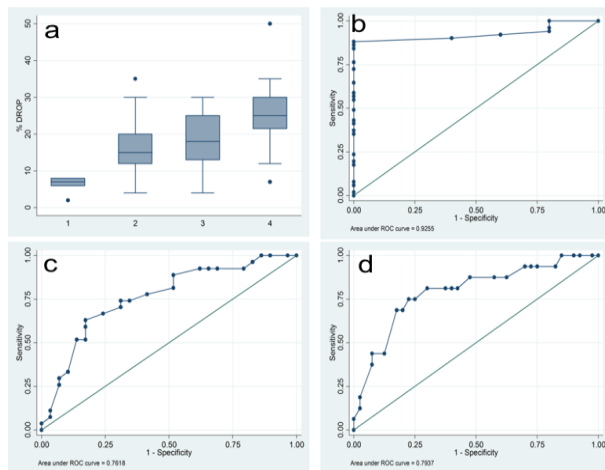
Figure 6.
a. Box plot showing distribution of percentage (%) drop values;
b. ROC curves showing % drop values for grade I v/s grade II;
c. ROC curves showing % drop values for grade II V/s grade III;
d. ROC curves showing % drop values for grade III V/s grade IV.

Comparision of ADC values and rCBV values for grading

The rCBV values were better than ADC values in differentiating grade I from grade II and grade II from grade III. The ADC values were better than rCBV values in differentiating grade III from grade IV as shown by comparison of AUC of ADC and maximum rCBV for different grades (Table 3).

Grades	AUC for ADC	AUC for rCBV
I vs II	0.8145	0.8538
II vs III	0.7905	0.8475
III vs IV	0.8706	0.7947

Table 3. Table showing AUC for ADC vs rCBV for different grades

Spectroscopy

Kruskal-Wallis equality-of-populations rank test showed a p value of 0.505 for NAA/Cr, 0.2058 for Cho/Cr, 0.6782 for Cho/NAA, 0.1275 for Cho+Cr/NAA and 0.5660 for NAA/Crn. Since the P value of all spectroscopy parameters were more than 0.05, these parameters were not significant in grading tumours. Hence the further statistical analysis was not done.

DISCUSSION

Therapeutic strategies, prognosis, and monitoring response to therapy depend on accurate grading of gliomas [4]. Gliomas, specially GBM exhibit both spatial and temporal heterogeneity which allows them to adapt quickly. Spatial heterogeneity leads to inadequate sampling of tumour at biopsy which may lead to error in classification. In two of our patients, temporal heterogeneity was evident as radiologically they were grade III while pathologically, they were grade II. Both the patients deteriorated within six months of diagnosis, hence pointing towards higher grade. This may have been due to sampling error during biopsy. Temporal heterogeneity leads to treatment failure and disease progression. One of our patients had grade I tumour transformed to Grade III in which ADC dropped from 1.2 to 0.8 x10-3mm2/s and rCBV increased from 1.1 to 3.2ml/100g. Patient remained stable for 4 years, after which there was increased frequency of seizures, refractory to drugs at which stage, MRI showed it to be grade III. The patient died after 1 year.

MR imaging can be used to grade astrocytomas into low-grade astrocytoma, anaplastic astrocytoma, and glioblastoma multiforme [5] and may help in management when the clinical course appears to be at odds with the neuropathologic diagnosis. Crossing midline, edema, signal heterogeneity, haemorrhage, border definition, cyst formation or necrosis and mass effect are some of the MRI features which can aid in predicting grade [6]. Necrosis was seen in 83.3% of glioblastoma multiforme (GBM) and 50% of anaplastic astrocytomas, irregular margins in 100% of GBM and anaplastic astrocytomas and haemorrhage in 55% of GBMs in our study. GBM most commonly showed edema (100%). Corpus callosum involvement was an indicator of higher grade. Conventional MR imaging, which depends on contrast enhancement, mass effect, edema, and necrosis for grading, is not always accurate for grading of gliomas. Contrast enhancement may be seen in some low grade gliomas while some high-grade tumours do not show enhancement. Advanced MR imaging techniques such as diffusion and perfusion imaging can help in such grading [5].

WHO formulated new guidelines in 2016 which emphasized integration of genetic make-up in classifying tumours. After conception of Radiogenomics Consortium in 2009, it is well known that distinct sub regions of tumours identifiable by MR imaging have distinct gene expression patterns [7,8]. Radiogenomics improved the diagnostic capability of even conventional MR imaging. Deep machine learning has increased the amount and accuracy of data by picking up subtle features that could not be picked up by even experienced radiologists. Age, gender, location, lateralization, signal intensity, enhancement pattern, surrounding edema and morphology of the tumour tell a lot about molecular subtypes and genetic profiling, based on which treatment selection, prognosis and follow-up can be decided. Ring like enhancement, large size with significant necrosis and temporal lobe (posterior subventricular, to be more precise) location suggest primary GBM, while frontal lobe location, homogeneous enhancement and young age suggest secondary GBM which has better prognosis [9]. The molecular subtypes of GBM are best predicted by edematous/tumour infiltrated volume and total tumour volume [10]. IDH-mutated gliomas can be differentiated from IDH wild type with 98% accuracy based on single lobe confinement, significant nonenhancing tumour, frontal lobe localization, large tumour size and presence of cysts and satellite lesions. MGMT methylated tumours show mixed nodular enhancement, small amount of edema, moderately elevated rCBV, and increased Ktrans [11]. Ring enhancement with necrosis suggest unmethylated MGMT-promoter region [12]. Frontal tumours are commoner in younger patients (<55 years) while elderly mostly have more posterior tumours [13]. This was clearly seen in our 40 year old patient with frontal tumour (Fig.1) and 58 year old patient with parietal tumour (Fig.3). Lower necrosis volume is seen in GBM in female patients. Higher necrosis volume in females predicted poor outcome [12]. GBMs in temporal lobe are likely to show EGFR amplification and EGFRv VIII mutation and show good effect of chemoradiation [12]. MGMT-methylated GBMs have predilection for left

hemisphere and MGMT- nonmethylated ones for right hemisphere [12]. In childhood brainstem gliomas, pontine involvement suggests high grade glioma (H3 K27 M mutant). Pilocytic astrocytoma, medulloblastoma {mainly sonic hedgehog (SHH) subtype or type 3} and atypical teratoid rhabdoid tumour (in less than 3 years of age) are the possibilities in posterolateral cerebellum [14]. Literature provides evidence that MGMT-methylated tumours show a lower volume of T2 abnormalities; a lower volume ratio of T2 abnormalities to contrast enhancement and central necrosis suggest a mesenchymal glioblastoma subtype and a sharp border makes a 1p19q-intact tumour more likely [11]. A multi institutional study of the cancer genome atlas (TCGA) GBM dataset by Gutman et al [15] demonstrated that proneural subtype showed low levels of contrast enhancement (reviewed in [9]).

Zinn et al [16] performed first comprehensive radiogenomic analysis using MRI volumetrics and gene and micro RNA expression profiling in GBM. They suggested that FLAIR is an imaging marker for edema and invasion and high FLAIR radiophenotypes may have a unique molecular tumour composition that leads to cellular migration and invasion [16]. By combining neuroimaging and DNA microarray analysis, multidimensional maps of gene-expression patterns in GBM were created. Diehn et al [17] hypothesized that underlying inter- and intratumoural gene-expression differences lead to phenotypic diversity of GBM which can be seen on neuroimaging. Unique imaging strategies could identify most of the gene expression signatures and hence radiophenotypes could be assessed more specifically by combining gene expression and MRI. There was significant complex and simple microvascular hyperplasia within contrast-enhancing regions which corresponded to a significant increase in rCBV and relative peak height (rPH) measurements. It was hypothesized that the enhancing and nonenhancing regions showed different gene expression patterns which was confirmed when 359 genes significantly overexpressed within contrast-enhancing samples were found to be associated with regulation of angiogenesis, proptosis and mitosis. Genes associated with cellular proliferative or infiltrative processes, hypoxia, and angiogenesis were upregulated in contrast enhancing tissues. Jain et al [18] showed that CBV and percentage signal (PS)

estimates in GBMs correlate positively with proangiogenic genes and inversely with anti angiogenic genes. Rao et al [19], combining transcriptional, post-transcriptional and signal transduction correlates of relative cerebral blood volume, revealed 326 genes, 76 miRNA and 8 proteins expressed between two phenotype classes- cell proliferation and angiogenesis associated pathways. Molecular examination of hemodynamic characteristics other than rCBV may shed further light on useful aspects and enhanced application of the technique for grading gliomas.

It would be interesting to investigate if there could be a way to find radioproteomic phenotypes functionally correlating with tumour imaging features in gliomas. Hobbs et al [20] studied correlation between gadolinium contrast-enhancement patterns on T1-weighted magnetic resonance (MR) images and spatial changes in protein expression profiles in GBM. Tissue samples from nonenhancing (NE) and contrast enhancing (CE) regions within a given tumour were compared. Proteins common to all individuals studied in both CE and NE regions were used as internal controls. The CE regions were extremely heterogeneous not only across the patients, but also within same patient while NE regions were comparably homogeneous. CE regions also contained more protein species than the NE region. The extracellular matrix in contrast-enhancing regions was likely to contain factors that presented increased permeability or microvessel density in neoplastic disease state. This shows that CE-MRI can guide proteomic analysis with SELDI-TOF-MS in GBM.

DWI assesses cellularity of tumours and ADC gives quantitative information about the restriction of water movement. Brain neoplasms with higher cellularity or with a higher grade show significantly low ADC values [21]. In our study, difference in the minimum ADC values for different grades of tumour was significant (P<0 .001), finding similar to those of Lee et al [22] and Kono et al [23] that high-grade gliomas show significantly low ADC values and increased signal intensity on DWI. Hilario et al [24] found that at a cut off ADC value of 1.185×10^{-3} mm2/s high and low grade gliomas could be differentiated with a sensitivity of 97.6% and specificity of 53.1%. Comparison between Hilario et al and our study is shown in Table 4. A lower cut off

value in our study has reduced the sensitivity but improved the specificity.

Study	Cut off ADC value (for low v/s high grade)	Sensitivity	Specificity
Hilario et al (2012)	1.185×10^{-3} mm^2/s	97.6 %	53.1 %
Our present study	0.75×10^{-3} mm^2/s	71.43 %	70 %

Table 4. Table comparing ADC values in differentiation of high and low-grade gliomas in various studies.

Fan et al [25] have demonstrated that ADC values in peritumoural regions were decreased compared to the contralateral normal white matter, but no significant difference was found as p value was more than 0.05. In our study also p value was more than 0.05 and hence was not a significant parameter for grading gliomas. Moreover the edema surrounding the glioma is vasogenic edema [6] which normally does not show diffusion restriction this may also be the reason that ADC in peritumoural edema is not very reliable in grading the tumours. DTI, a method of visualizing the anisotropy of proton motion, may eliminate the partial volume effect of peritumoural edema, and may highlight the difference between high-grade and low-grade gliomas [26]. Zinn et al [27] described Diffusion Weighted magnetic resonance imaging radiophenotypes and associated molecular pathways in glioblastoma. Given that dMRI and ADC reflect tumour cellularity and a high N:C ratio in niches of restricted diffusion, authors hypothesized that dMRI signal intensity beyond the region of enhancement could identify GBMs that were highly infiltrative within nonenhancing peritumoural FLAIR area. Gene expression profiles associated with restricted diffusion in the peritumoural dMRI-FLAIR niche in GBM was examined which showed consistent upregulation of BMI1, a known regulator of stemlike states in cancer cells and is associated with migration, invasion and poor prognosis. Likewise, significant negative correlation has been shown between ADC and 2-hydroxyglutarate (2-HG) levels, a metabolite found in IDH mutated tumours [9], which suggests that ADC may be decreased in IDH-mutated tumours. Methylated tumours display features of lower cellularity (high minimum ADC ratio and low minimum FA ratio) [11]. Heiland et al [28]

found that in enhancing tumour region, FA directly correlated with activation of epithelial-to-mesenchymal transition pathway. Hence high FA predicted worse prognosis in GBM, while higher MD predicted good prognosis.

Tumour growth depends largely on new blood vessel growth. Simple diffusion of oxygen, nutrients and other essential materials can support tumour growth only upto a size of 1-2mm3 beyond which neoangiogenesis is necessary. Metastasis also cannot occur without growth of new blood vessels [29]. Contrast enhancement occurs due to leakage of contrast and thus CE-MRI highlights only the blood brain barrier (BBB) disruption. On the other hand, perfusion study is based upon blood flow at capillary level. It tells about the capillary network and hence shows the degree of neoangiogenesis [30]. As the tumour growth and hence its grade depends on neoangiogenesis rather than on leakage of BBB, perfusion MRI is an earlier and better predictor of grade than contrast enhancement. Moreover, due to its ability to pick up areas of angiogenesis, PWI imaging has capacity to direct stereotactic biopsy to such areas (which have a higher grade) in an otherwise heterogeneous tumour, thus avoiding understaging of the tumour, specially in cases of non-enhancing gliomas which have comparatively intact BBB [31]. The drawback is that in cases of high grade enhancing gliomas, there is significant BBB breakdown leading to leakage of contrast in extravascular space during first pass of contrast and reduced susceptibility effects between intra and extravascular compartments in this area leading to underestimation of tumour vascularity and hence grade [32]. Peritumoural areas in anaplastic tumours show altered capillary morphology as well as tumour cells along newly formed or preexisting dilated vessels while low grade gliomas have less infiltrating tumour cells. This is reflected in elevated blood volume before enhancement. Vascularity related heterogeneity of peritumoural region as shown on PWI can be helpful in better estimation of true brain tumour size pre-operatively [33].

Although preoperative grading of gliomas is mainly done by DWI and PWI, there are only few studies validating the usefulness of diffusion and perfusion MRI solely in non-enhancing gliomas. Fan et al [25] hypothesized that DWI/PWI could provide additional useful information in the assessment and tumour grading of supratentorial glial neoplasms,

which lacked contrast enhancement on preoperative neuroimaging and therefore evaluated the usefulness of diffusion/perfusion-weighted MRI in patients with non-enhancing supratentorial brain gliomas. Both solid portions as well as peritumoural regions of anaplastic gliomas showed high rCBV ratios but low grade gliomas did not [25]. So it was concluded that higher rCBV ratios in both solid portions and peritumoural regions correlate significantly with anaplasia. In our study rCBV in peritumoural edema was not significant (p = 0.13). Comparison of cut off rCBV values within the tumour between various studies is shown in Table 5. Spampinato et al [32] demonstrated best sensitivity and specificity for differentiating low and high grades, at a cut off of 2.14 ml/100 g. We also found best sensitivity and specificity at a cut off of 2.6 ml/100 g which is quite close to 2.1 ml/100 g though our sensitivity and specificity were less than that of Spampinato. This difference may be explained on the basis of different number of cases in two studies and because our study contained mix of astrocytoma and oligodendroglioma while Spampinato's study had only oligodendroglioma. Sensitivity of all the studies is comparable. The difference in specificity arises due to different cut off values of rCBV for low v/s high grade tumours. Near cut off of 1.75 ml/100 g, both Law et al [34] and Hilario et al [24] had a specifity of 50-60%. At a cut off of 3.3 ml/100 g, Roy et al [35] showed specificity of 88%. At a cut off of 2.6ml/100mg our specificity was 76.47% which is in between the above values (cut off is also in between the two) and hence in sync with previous studies.

Study	Cut off rCBVvalue (ml/100 g)	Sensitivity (%)	Specificity (%)
Law et al(2003)	1.75	95.0	57.5
Weber et al(2006)	1.6	94	78
Aprile et al(2012)	3.5	79.4	95.8
Hilario et al(2012)	1.74	94.4	50.0
Roy et al(2013)	3.34	100	88
Spampinato et al(2007)	2.14	100	86
Shin et al	3.57	72.7	100
Our present study	2.6	76.67	76.47

Table 5. Table comparing rCBV values within the tumor in differentiation of high and low grade gliomas in various studies.

Ellingson [13] based on his decades of work examined association between radiological and histological features in Glioblastoma. He comprehensively reviewed anatomical imaging pathology associations, association between tumour size, location and molecular characteristics, diffusion and perfusion MRI pathology correlation and quantification of intuitive radiographic features. Maximum rCBV is considered to be a significant predictor of mean vessel diameter. Smits and Bent [11] found that methylated tumours show less perfusion and increased volume transfer constant (Ktrans) than unmethylated tumours. Though pseudoprogression is seen commonly, but progression time is significantly longer in patients with MGMT-promoter methylation compared with the unmethylated group, both of which may be due to increased Ktrans, i.e., permeability in methylated group which leads to contrast leakage (seen as pseudoprogression) and better drug delivery (prolonging progression) [10]. Thus increase in enhancement within three months after completion of radiotherapy in patients with MGMT methylated tumours should be suspected as pseudoprogression rather than progressive disease. This shows how amalgamation of imaging and genomics can reinforce each other. Imaging can help in predicting tumour genetics, while genetic profile helps in cautious interpretation of post-treatment enhancement in terms of progression vs pseudoprogression. Oligodendroglioma have comparatively higher rCBV regardless of grade on histology [13]. PWI can differentiate pilocytic astrocytoma (rCBVmax = 1.19±0.71)from hemangioblastoma (rCBVmax = 9.37±2.37) [14]. Vajepeyam et al have shown that ADC histogram metrics combined with permeability metrics differentiate low and high-grade pedistric brain tumours with high accuracy [14].

Bulakbasi et al [33, 36] studied usefulness of MR spectroscopy and ADC calculation for tumour grading. They found that though MR spectroscopy could not be of much help in grading malignant tumours, it could help to differentiate benign from malignant tumours [36]. In our study also spectroscopy was not helpful in grading of gliomas. Hsu et al [37] correlated metabolite ratios with histopathologic grading in 27 patients with cerebral gliomas. They concluded that there was no significant metabolite difference between grade III and grade IV tumours (p>0.1), or significant difference in lactate occurrence rates among

different grades (p = 0.26). Though the metabolite ratios in our study were not helpful quantitatively in grading of gliomas, presence of some peaks like lipid and lactate did help in grading. Poptani et al [38] and Hsu et al [37] stated that lactate peak can be found in all grades of tumours. In our study also lactate peak was found in almost all the grades though with more frequency in higher grades.

Radiogenomics focused on spectroscopic parameters may also aid in predicting molecular profiling of tumours. GBM harboring IDH1 mutation show 2-hydroxyglutarate (2-HG) on MR spectroscppy [9]. So 2-HG level can be a predictor of IDH1 mutation, but is not universally available in standard MR equipments at present, but is definitely a way forward. Likewise, oligodendrocytic tumours correlated with N-acetylaspartate metabolite, high creatine metabolite (nCr) was seen in proneural GBM subtype, and low nCr predicted mesenchymal subtype; low nGlx predicted neural subtype, and its high value suggested classical subtype [10]. A high peak of choline can help differentiate atypical laminated medulloblastoma from Lhermitte-Duclos disease which are difficult to differentiate on morphology alone [14].

Brain shift during surgery often leads to incongruence in tumour borders assessed by pre-operative and operative MRI. Some tumours show false-positive contrast enhancement and small molecule Gd-agents may also spread from the initial area of tumour enhancement into the peritumoural zone of edema over time. This leads to inaccuracies in assessment of tumour extent. Multimodality approach has been suggested to overcome this shortcoming and to assess true tumour extent. The focus in recent past has been on exploring optical methods which may be based on either intrinsic tissue properties or by using exogenous contrast agents. Nevertheless, small field of view, decreased specificity due to auto fluorescence, and rapid photobleaching pose challenges in using these optical procedures. Some other useful methods for defining tumour margins include fluorescence-guided resection of malignant gliomas using 5-aminolevulinic acid (body's own metabolite in heme biosynthesis pathway and metabolic marker of malignant cells which is converted into fluorescent porphyrins in cells) as marker [39] and Desorption Electrospray Ionization Mass Spectrometry (DESI-MS) imaging based on lipid patterns for intra

operative molecular characterization of brain tumours [40]. Using mouse model of Glioblastoma, Huang et al have reported integrin –targeted SERRS nanoparticles to depict the true tumour extent. Method bears fairly high potential for clinical translation for glioma grading in humans [41].

Various radiological parameters can also predict prognosis with fair degree of accuracy. While performing an integrative network-based analysis of magnetic resonance spectroscopy and genome wide expression in glioblastoma multiforme, Heiland et al [42] found that patients with higher nNAA (N-Acetyl Aspartate) showed longer progression free survival (reviewed in [10]). Patients with highly perfused low grade tumours fared worse than patients with lowly perfused high grade tumours. IDH-mutated tumours fare much better than IDH wild type of same grade. Limited peritumoural edema predicted better prognosis in patients with methylated glioblastoma specifically [11]. Mutations in the promoter for telomerase reverse transcriptase (TERT), an enzyme that elongates telomeres, have been associated with a worse prognosis in both IDH mutant and IDH wild-type GBMs. Increased amounts of Ki-67, a cellular protein associated with proliferation and present in many tumours, is also associated with a worse prognosis [43].

Even choice of chemotherapy can be improved with radiogenomics approach. GBM with proneural signature had better outcome when bevacizumab was given from initiation of therapy. Mesenchymal phenotype responded better when bevacizumab was given at recurrence, but not when given as first line along with radiation and temozolomide [13]. The MGMT unmethylated group responded only to radiotherapy [10]. siRNA can transduce previously TMZ-resistant glioma-initiating cells, enhancing their chemosensitivity against TMZ [12]. Co-deletion of chromosomal arms 1p and 19q predict favorable outcome and sensitivity to chemotherapy respectively.

There are some major issues with universal application of conventional radiogenomics at present. These are overlap of MRI features between different mutations, several mutations like IDH, MGMT, and TP53, occuring in tandem, intratumoural heterogeneity with different portions of the tumour having different genetic and imaging features. Machine learning is better as it does objective quantitative evaluation and can detect subtle voxel-

level patterns [43]. So a combination of conventional and machine learning based radiogenomics has huge potential towards accurate diagnosis, classification, grading, prognosticating, selecting adequate therapy, monitoring therapy, identifying early therapy failure and modifying therapy accordingly in cases of glioma, i.e., it is the way forward in theranostics and has the potential to replace invasive and non-representative biopsies as it gives the total overview of the tumour.

Our study has some limitations. Stereotactic biopsies were not targeted according to rCBV or ADC maps. So there is possibility of histopathologic misdiagnosis attributable to sampling error in the pathologic examination because of the histologic heterogeneity of tumour tissues. Only elementary radiogenomics based approach could be followed as the facility for MR based stereotactic biopsies and advanced machine learning facilities do not exist at our place. Ongoing radiological, molecular profiling and proteomic studies in our laboratories are focused on providing additional translational tools to decipher MR, genomic and proteomic characteristics of gliomas to better grade them.

CONCLUSION

Both maximum rCBV and minimum ADC values within the tumour were useful in grading gliomas, but both these values in peritumoural edema were not significant in grading gliomas. rCBV values were better than ADC values in differentiating grade I from II and grade II from III. The ADC values were better than rCBV values in differentiating grade III from grade IV. The metabolite ratios were not helpful in grading of gliomas, but presence of some peaks like lipid and lactate did help in grading. Lactate peak was found in almost all the grades (except grade I) though with more frequency in higher grades. Presence of lipids suggested a higher grade of malignancy. Radiogenomics coupled with multimodality radiomic procedures can further improve the accuracy of grading.

ETHICAL CONSIDERATIONS

The study was carried out in accordance to standards of the institutional ethics committee and with the 1964 Helsinki declaration.

REFERENCES

1. Okaili, R. N., Krejza, J., Wang, S., Woo, J. H., Melhem, E. R. (2006). Advanced MR Imaging Techniques in the Diagnosis of Intraaxial Brain Tumors. RadioGraphics, 26, S173-89.

2. Jansen, R. W., van Amstel, P., Martens, R. M., Kooi, I. E., Wesseling, P., de Langen, A. J., van Oordt, C. W. M. V. H., Jansen, B. H. E., Moll, A. C., Dorsman, J. C., Castelijns, J. A., de Graaf, P., de Jong, M. C. (2018). Non-invasive tumor genotyping using radiogenomic biomarkers, a systematic review and oncology-wide pathway analysis. Oncotarget, 9(28), 20134 - 20155.

3. Seow, P., Wong, J. H. D., Ahmad-Annuar, A., Mahajan, A., Abdullah, N. A., Ramli, N. (2018). Quantitative magnetic resonance imaging and radiogenomic biomarkers for glioma characterisation: a systematic review. Br J Radiol, 91(1092), 20170930.

4. Schwartzbaum, J. A., Fisher, J. L., Aldape, K. D., Wrensch, M. (2006). Epidemiology and molecular pathology of glioma. Nat Clin Pract Neurol, 2(9), 494-503.

5. Kernohan, J. W., Mabon, R. F., Svien, H. J. et al (1995). Neuroepithelial tumors of the adult brain. In: Youmans. Neurological Surgery. 4th edition. Philadelphia: W.B. Saunders Co, 2612-84.

6. Chishty, I. A., Rafique, M. Z., Hussain, M., Akhtar, W., Ahmed, M. N., Sajjad, Z., Ali, S. Z. (2010). MRI Characterization and Histopathological Correlation of Primary Intra -axial Brain Glioma. JLUMHS, 9(2), 64-69.

7. Van Meter, T., Dumur, C., Hafez, N., Garrett, C., Fillmore, H., Broaddus, W. C. (2006). Microarray analysis of MRI-defined tissue samples in glioblastoma reveals differences in regional expression of therapeutic targets. Diagn Mol Pathol, 15(4), 195–205.

8. Kuo, M. D., & Jamshidi, N. (2014). Behind the numbers: Decoding molecular phenotypes with radiogenomics-guiding principles and technical considerations. Radiology, 270(2), 320-5.

9. ElBanan, M. G., Amer, A. M., Zinn, P. O., Colen, R. R. (2015). Imaging genomics of Glioblastoma: state of the art bridge between genomics and neuroradiology. Neuroimaging Clin N Am, 25(1), 141-53.

10. Kazerooni, F. A., Bakas, S., Rad, H. S., Davatzikos, C. (2020). Imaging signatures of glioblastoma molecular characteristics: A radiogenomics review. J Magn Reson Imaging, 52(1):54-69.

11. Smits, M., & van den Bent, M. J. (2017). Imaging Correlates of Adult Glioma Genotypes. Radiology, 284(2), 316-31.

12. Moton, S., Elbanan, M., Zinn, P. O., Colen, R. R. (2015). Imaging Genomics of Glioblastoma: Biology, Biomarkers, and Breakthroughs. Top Magn Reson Imaging, 24(3), 155-63.

13. Ellingson, B. M. (2015). Radiogenomics and imaging

phenotypes in glioblastoma: novel observations and correlation with molecular characteristics. Curr Neurol Neurosci Rep, 15(1), 506.

14. Kerleroux, B., Cottier, J. P., Janot, K., Listrat, A., Sirinelli, D., Morel, B. (2020). Posterior fossa tumors in children: Radiological tips & tricks in the age of genomic tumor classification and advance MR technology. J Neuroradiol, 47(1), 46-53.

15. Gutman, D. A., Cooper, L. A., Hwang, S. N., Holder, C. A., Gao, J., Aurora, T. D., Dunn, W. D. Jr,Scarpace, L., Mikkelsen, T., Jain, R., Wintermark, M., Jilwan, M., Raghavan, P., Huang, E., Clifford, R. J., Mongkolwat, P., Kleper, V., Freymann, J., Kirby, J., Zinn, P. O., Moreno, C. S., Jaffe, C., Colen, R., Rubin, D. L., Saltz, J., Flanders, A., Brat, D. J. (2013). MR imaging predictors of molecular profile and survival: multi-institutional study of the TCGA glioblastoma data set. Radiology, 267(2), 560-9.

16. Zinn, P. O., Majadan, B., Sathyan, P., Singh, S. K., Majumder, S., Jolesz, F. A., Colen, R. R. (2011). Radiogenomic mapping of edema/cellular invasion MRI-phenotypes in glioblastomamultiforme. PLoS One, 6(10), e25451.

17. Diehn, M., Nardini, C., Wang, D. S., McGovern, S., Jayaraman, M., Liang, Y., Aldape, K., Cha, S., Kuo, M. D. (2008). Identification of noninvasive imaging surrogates for brain tumor gene-expression modules. Proc Natl Acad Sci, 105(13), 5213-8.

18. Jain, R., Poisson, L., Narang, J., Scarpace, L., Rosenblum, M. L., Rempel, S., Mikkelsen, T. (2012). Correlation of perfusion parameters with genes related to angiogenesis regulation in glioblastoma: a feasibility study. Am J Neuroradiol, 33(7), 1343-8.

19. Rao, A., Manyam, G., Rao, G., Jain, R. (2016). Integrative Analysis of mRNA, microRNA, and Protein Correlates of Relative Cerebral Blood Volume Values in GBM Reveals the Role for Modulators of Angiogenesis and Tumor Proliferation. Cancer Inform, 15, 29-33.

20. Hobbs, S. K., Shi, G., Homer, R., Harsh, G., Atlas, S. W., Bednarski, M. D. (2003). Magnetic resonance image-guided proteomics of human glioblastoma multiforme. J Magn Reson Imaging, 18(5), 530-6.

21. Louis, D. N., Ohgaki, H., Wiestler, O. D., Cavenee, W. K., Burger, P. C., Jouvet, A., Scheithauer, B., W., Kleihues, P. (2007). The 2007 WHO classification of tumours of the central nervous system. Acta Neuropathol, 114(2), 97-109.

22. Lee, E. J., Lee, S. K., Agid, R., Bae, J. M., Keller, A., Terbrugge, K. (2008). Preoperative grading of presumptive low-grade astrocytomas on MR imaging: diagnostic value of minimum apparent diffusion coefficient. Am J Neuroradiol, 29(10), 1872-7.

23. Kono, K., Inoue, Y., Nakayama, K., Shakudo, M., Morino, M., Ohata, K., Wakasa, K., Yamada, R. (2001). The role of diffusion-weighted imaging in patients with brain tumors. Am J Neuroradiol, 22(6), 1081-8

24. Hilario, A., Ramos, A., Perez, N., Salvador, E., Millan, J. M., Lagares, A., Sepulveda, J. M., Leon, G., Lain, H., Ricoy, J. R.

(2012). The Added Value of Apparent Diffusion Coefficient to Cerebral Blood Volume in the Preoperative Grading of Diffuse Gliomas. Am J Neuroradiol, 33(4), 701-7.

25. Fan, G. G., Deng, Q. L., Wu, Z. H., Guo, Q. Y. (2006). Usefulness of diffusion/perfusion-weighted MRI in patients with non-enhancing supratentorial brain gliomas: a valuable tool to predict tumor grading. British J Radiology, 79, 652–8.

26. Lu, S., Ahn, D., Johnson, G., Law, M., Zagzag, D., Grossman, R. I. (2004). Diffusion-tensor MR imaging of intracranial neoplasia and associated peritumoral edema: introduction of the tumor infiltration index. British J Radiology, 232, 221–8.

27. Zinn, P. O., Hatami, M., Youssef, E., Thomas, G. A., Luedi, M. M., Singh, S. K., Colen, R. R. (2016). Diffusion Weighted Magnetic Resonance Imaging Radiophenotypes and Associated Molecular Pathways in Glioblastoma. Neurosurgery, 63(Suppl 1), 127-35.

28. Heiland, D. H., Simon-Gabriel, C. P., Demerath, T., Haaker, G., Pfeifer, D., Kellner, E., Kiselev, V. G., Staszewski, O., Urbach, H., Weyerbrock, A., Mader, I. (2017). Integrative Diffusion-Weighted Imaging and Radiogenomic Network Analysis of Glioblastoma multiforme. Sci Rep, 7, 43523.

29. Bello, L., Giussani, C., Carrabba, G., Pluderi, M., Costa, F., Bikfalvi, A. (2004). Angiogenesis and invasion in gliomas. Cancer Treat Res, 117, 263–84.

30. Batra, A., Tripathi, R. P., Singh, A. K. (2004). Perfusion magnetic resonance imaging and magnetic resonance spectroscopy of cerebral gliomas showing imperceptible contrast enhancement on conventional magnetic resonance imaging. Australas Radiol, 48(3), 324–32.

31. Maia, A. C. M., Malheiros, S. M. F., da Rocha, A. J., da Silva, C. J., Gabbai, A. A., Ferraz, F. A. P., Stavale, J. N. (2005). MR cerebral blood volume maps correlated with vascular endothelial growth factor expression and tumor grade in non enhancing gliomas. Am J Neuroradiol, 26, 777-83.

32. Spampinato, M. V., Smith, J. K., Kwock, L., Ewend, M., Grimme, J. D., Camacho, D. L. A., Castillo, M. (2007). Cerebral Blood Volume Measurements and Proton MR Spectroscopy in Grading of Oligodendroglial Tumors. Am J Neuroradiol, 188, 204–12.

33. Bulakbasi, N., Kocaoglu, M., Farzaliyev, A., Tayfun, C., Ucoz, T., Somuncu, I. (2005). Assessment of diagnostic accuracy of perfusion MR imaging in primary and metastatic solitary malignant brain tumors. Am J Neuroradiol, 26(9), 2187–99.

34. Law, M., Yang, S., Wang, H., Babb, J. S., Johnson, G., Cha, S., Knopp, E. A., Zagzag, D. (2003). Glioma grading: sensitivity, specificity andpredictive values of perfusion MR imaging and proton MR spectroscopic imaging compared with conventional MR imaging. Am J Neuroradiol, 24(10), 1989-98.

35. Roy, B., Gupta, R. K., Maudsley, A. A. et al (2013). Utility of multiparametric 3-T MRI for glioma characterisation. Neuroradiology, 55, 603 -13.

36. Bulakbasi, N., Kocaoglu, M., Ors, F., Tayfun, C., Ucoz, T.

(2003). Combination of Single-Voxel Proton MR Spectroscopy and Apparent Diffusion Coefficient Calculation in the Evaluation of Common Brain Tumors. Am J Neurodiol, 24(2), 225-33.

37. Hsu, Y. Y., Chang, C. N., Wie, K. J., Lim, K. E., Hsu, W. C., Jung, S. M. (2004). Proton Magnetic Resonance Spectroscopic Imaging of Cerebral Gliomas: Correlation of Metabolite Ratios with Histopathologic Grading. Chang Gung Med J, 27(6), 399-407.

38. Poptani, H., Gupta, R. K., Roy, R., Pandey, R., Jain, V. K., Chhabra, D. K. (1995). Characterization of Intracranial Mass Lesions with In Vivo Proton MR Spectroscopy. Am J Neuroradiol, 16, 1593-603.

39. Tonn, J. C., & Stummer, W. (2008). Fluorescence-guided resection of malignant gliomas using 5-aminolevulinic acid: Practical use, risks, and pitfalls. Clin Neurosurg, 55, 20-6.

40. Eberlin, L. S., Norton, I., Orringer, D., Dunn, I. F., Liu, X., Ide, J. L., Jarmusch, A. K., Ligon, K. L., Jolesz, F. A., Golby, A. J., Santagata, S., Agar, N. Y. R., Cooks, R. G. (2013). Ambient mass spectrometry for the intraoperative molecular diagnosis of human brain tumors. Proc Natl Acad Sci, 110(5), 1611-6.

41. Huang, R., Harmsen, S., Samii, J. M., Karabeber, H., Pitter, K. L., Holland, E. C., Kircher, M. F. (2016). High Precision Imaging of Microscopic Spread of Glioblastoma with a Targeted Ultrasensitive SERRS Molecular Imaging Probe. Theranostics, 6(8), 1075-84.

42. Heiland, D. H., Mader, I., Schlosser, P., Pfeifer, D., Carro, M. S., Lange, T., Schwarzwald, R., Vasilikos, I, Urbach, H., Weyerbrock, A. (2016). Integrative network-based analysis of magnetic resonance spectroscopy and genome wide expression in glioblastoma multiforme. Sci Rep, 6, 29052.

43. Chow, D., Chang, P., Weinberg, B. D., Bota, D. A., Grinband, J., Filippi, C. G. (2018). Imaging Genetic Heterogeneity in glioblastoma and Other Glial Tumors: Review of Current Methods and Future Directions. Am J Roentgenol, 210(1), 30-38.